Geological Society, London, Special Publications

Denudation along the Atlantic passive margin: new insights from apatite fission-track analysis on the western coast of South Africa

A. Kounov, G. Viola, M. de Wit and M. A. G. Andreoli

Geological Society, London, Special Publications 2009; v. 324; p. 287-306
doi:10.1144/SP324.19

Notes

Denudation along the Atlantic passive margin: new insights from apatite fission-track analysis on the western coast of South Africa

A. KOUNOV[1]*, G. VIOLA[2], M. DE WIT[3] & M. A. G. ANDREOLI[4]

[1]*Institute of Geology and Paleontology, Basel University, 4056 Basel, Switzerland*

[2]*NGU, Geological Survey of Norway, 7491 Trondheim, Norway*

[3]*AEON and Department of Geological Sciences, UCT, 7701 Rondebosch, South Africa*

[4]*South African Nuclear Energy Corporation, PO Box 582, 0001 Pretoria, South Africa, and School of Geosciences, University of the Witwatersrand, Private Bag 3, 2050 Wits, South Africa*

**Corresponding author (e-mail: a.kounov@unibas.ch)*

Abstract: Apatite fission-track (AFT) data from two traverses across the Great Escarpment of the western coast of South Africa are used to reconstruct the tectonic evolution and denudation history of this sector of the Atlantic passive margin. Fission-track ages range between 180 and 86 Ma. Modelling of this data identifies two distinct cooling events. The first event, between 160 and 138 Ma, is recorded only by the rocks above the escarpment in the Karoo area, and is tentatively linked to post-Karoo magmatism (*c.* 180 Ma) thermal relaxation. The second, between 115 and 90 Ma, results instead from a tectonically induced denudation episode responsible for the removal of up to 2.5 km of crust across the coastal zone in front of the escarpment and less than 1 km on the elevated interior plateau. Based on these results, it is suggested that the Cretaceous is the time when most of the elevated topography of Southern Africa was generated, with only a minor Cenozoic contribution.

Continental passive margins have been the target of geomorphological studies since the early 1920s and different models have been suggested for their morphotectonic development (e.g. du Toit 1926; King 1953; Ollier 1985; Partridge & Maud 1987; Gilchrist & Summerfield 1990). Passive margins with high elevation have been of particular interest due to their impressive geomorphological features, including a low-lying coastal plain separated from an elevated inland region by seaward-facing escarpments. In the early schemes of margin evolution, the formation of the escarpment was generally attributed to the downflexing of the lithosphere and the development of a broad monocline that was subsequently eroded by backwearing during successive denudational phases (e.g. King 1953; Ollier 1985; Ollier & Marker 1995; Partridge & Maud 1987; Seidl *et al.* 1996). This type of evolutionary model relied mostly on geomorphological observations and on the correlation of erosional surfaces over great distance. The main problem with these models, however, is the lack of reliable age constraints on the erosion surfaces and quantitative information about the rates of denudation, which in turn hamper reliable large-scale correlations.

Over the past two decades a number of low-temperature thermochronological studies, including apatite fission-track (AFT), (U–Th)/He and cosmogenic nuclide analysis, have provided new quantitative geochronological constraints on the denudational history of passive margins, thus allowing the testing of earlier evolutionary models (e.g. Moore *et al.* 1986; Brown *et al.* 1990, 2000; Gallagher *et al.* 1998; Gallagher & Brown 1999; Fleming *et al.* 1999; Cockburn *et al.* 2000; Persano *et al.* 2002; Kounov *et al.* 2007, 2008). AFT and (U–Th)/He thermochronology are of particular value when attempting to understand the morphotectonic history of continental margins because these methods provide quantitative estimates of the amount of rock removal in the upper *c.* 3–5 km of the continental crust over timescales of millions to hundreds of millions of years. This in turn allows the reconstruction of the early denudation stages, whereas later short-term and more site-specific erosional processes and their rates are better studied with measurements of *in situ*-produced cosmogenic nuclides.

Based on these recent geochronological advances, new conceptual models have been proposed that differ from the classical escarpment retreat (backwearing) schemes essentially in the character of the post-break-up tectonics, the initial position and subsequent migration of the drainage divide, and in the spatial and temporal pattern of related denudation (e.g. Gilchrist & Summerfield 1990; Gilchrist *et al.* 1994; Cockburn *et al.* 2000; Brown *et al.* 2002).

From: LISKER, F., VENTURA, B. & GLASMACHER, U. A. (eds) *Thermochronological Methods: From Palaeotemperature Constraints to Landscape Evolution Models*. Geological Society, London, Special Publications, **324**, 287–306.
DOI: 10.1144/SP324.19 0305-8719/09/$15.00

The regional patterns of post break-up denudation along the continental margin of Southern Africa, as reconstructed from several AFT and cosmogenic nuclides studies, are generally incompatible with a simple model of landscape development involving steady retreat of an escarpment initially formed at the coast at the time of break-up (e.g. Fleming *et al.* 1999; Brown *et al.* 2000, 2002; Cockburn *et al.* 2000; Van der Wateren & Dunai 2001; Kounov *et al.* 2007, 2008; Tinker *et al.* 2008). Reported denudation rates along the coastal plain since the break-up are an order of magnitude lower than the values necessary for the escarpment retreat model.

These recent geochronological data require, instead, more complex models whereby the escarpment that formed at the coast at the time of the continental break-up was rapidly destroyed by rivers flowing from an interior divide towards the rapidly changing base level (Cockburn *et al.* 2000; Brown *et al.* 2002). This interpretation is in agreement with numerical models of surface evolution that emphasize the importance of drainage divides in controlling the location and evolution of major escarpments (e.g. Gilchrist *et al.* 1994; van der Beek & Braun 1999). More recently, however, these numerical models were criticized by Moore & Blenkinsop (2006), based on field observations that apparently support a scarp retreat model for the evolution of the Drakensberg escarpment (cf. King 1953). Thus, the details of the evolution of the great southern African escarpment still remain elusive.

Detailed AFT analyses on outcrop and borehole samples from the South African margin suggest the presence of a first period of accelerated denudation in the early Cretaceous (140–120 Ma) followed by a second in the Mid-Cretaceous (100–80 Ma: Brown *et al.* 2002; Tinker *et al.* 2008). A Late Cretaceous episode of accelerated denudation (80–60 Ma) was reported from the Drakensberg Escarpment area (Brown *et al.* 2002), whereas Raab *et al.* (2002) suggest a discrete period of accelerated cooling, beginning at about 70 Ma, in northern Namibia related to the reactivation of earlier basement structures (e.g. the Waterberg thrust), possibly caused by changes in the spreading geometry in the South Atlantic and SW Indian Ocean (e.g. Nürnberg & Müller 1991).

These studies indicate in general that a total of approximately 5 km of rocks were eroded during the Cretaceous, whereas during the Cenozoic the amount of total denudation decreased dramatically to less than about 1 km, approaching the present-day denudation rates as determined from cosmogenic nuclides data (Fleming *et al.* 1999; Cockburn *et al.* 2000; Van der Wateren & Dunai 2001; Kounov *et al.* 2007).

Whereas the southern (Tinker *et al.* 2008) and the eastern (Brown *et al.* 2002) coast of South Africa were already investigated by detailed AFT studies with the goal of understanding the local evolution and denudation history, the Atlantic passive margin along the west coast remains poorly studied. Our AFT work contributes further to the understanding of the Atlantic African margin by providing a new, detailed reconstruction of the spatial and temporal patterns of denudation along two transects across the western passive margin of South Africa and its interior since the onset of continental rifting.

The western margin of South Africa

Summary geological framework

The western coast of South Africa is characterized by the occurrence of diverse lithologies, from Proterozoic metamorphic rocks to Neoproterozoic and Mesozoic sedimentary and igneous successions. The Mesoproterozoic Namaqualand Metamorphic Province comprises intensely deformed supracrustal sequences intruded by numerous pre-, syn- and post-tectonic granitoids (e.g. Johnson *et al.* 2006). Exhumation of the Namaqualand metamorphic rocks during the Early Neoproterozoic (between 1000 and 800 Ma) was followed by deposition of the Gariep Supergroup in a pull-apart basin (Gresse 1995). The sediments of the Neoproterozoic–Cambrian Vanrhynsdorp Group unconformably overlie the Gariep Supergroup (Johnson *et al.* 2006). The Vanrhynsdorp and Gariep Group rocks were deformed and metamorphosed during the Pan-African orogeny between 650 and 480 Ma at relatively low temperatures. Proterozoic and Neoproterozoic rocks are unconformably overlain by the Ordovician–Devonian thick siliciclastic sequences of the Cape Supergroup (Johnson *et al.* 2006). In the study area the Cape Supergroup is represented mainly by the quartzite-dominated rocks of the Table Mountain Group (Johnson *et al.* 2006) (Fig. 1). From the late Carboniferous to the Early Jurassic, the Karoo sedimentary succession (Karoo Supergroup), which consists of several kilometres of clastic sediments, was deposited in the Karoo Basin. This is considered as a foreland basin possibly formed in response to orogenic loading of the Cape Fold Belt to the south (Johnson *et al.* 2006). The Cape Fold Belt formed during crustal shortening related to the subduction and accretion of the paleo-Pacific plate beneath Gondwana (de Wit & Ransome 1992). The break-up of Gondwana (*c.* 170–150 Ma: Hawkesworth *et al.* 1999) started with the separation of west Gondwana (Africa and South America) from east Gondwana (Australia, Antarctica, India and New Zealand), post-dating the extrusion of the

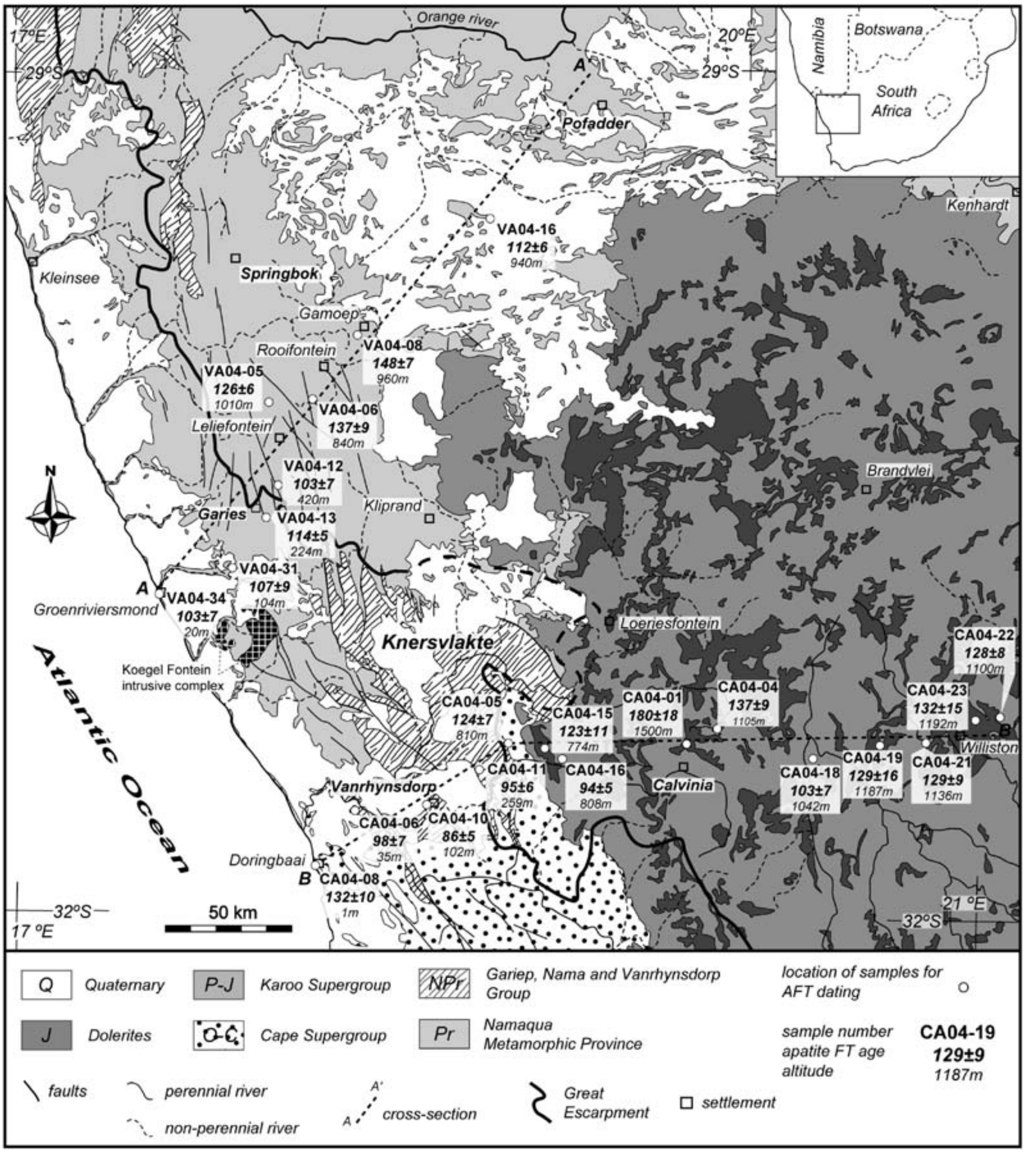

Fig. 1. Geological map of the study area (western South Africa) with the locations of the analysed samples and obtained fission-track ages. Lines A–A′ and B–B′ trace the sections of Figure 4.

voluminous and extensive continental flood basalts of the Drakensberg Group (184–174 Ma: Jourdan *et al.* 2007) exposed in the SW part of South Africa and with the emplacement of numerous dolerite sills (Karoo magmatics) preferentially intruded into the flat-lying beds of the Karoo Supergroup (Cox 1992; Duncan *et al.* 1997). Continental rifting between South America and Africa began during the Late Jurassic (*c.* 150 Ma: Nürnberg & Müller 1991; Stern & de Wit 2004; Trumbull *et al.* 2007). The rifting was accompanied by the intrusion of syenite and granite plutons, as well as dolerite dykes, between 137 and 125 Ma along the margin (e.g. Eales *et al.* 1984; Trumbull *et al.* 2007). One prominent intrusion is the Rietport granite, part of the Koegel Fontein intrusive complex (133.9 $\pm$ 1.3 Ma: De Beer *et al.* 2002), now cropping out to the NW of Vanrhynsdorp (Fig. 1).

The rifting–drifting transition was marked by the initiation of sea-floor spreading in the southern Atlantic at about 134 Ma (Rabinovich & LaBrecque 1979; Eagles 2007). The southern Atlantic opened by northwards propagation of the spreading centre over a period of around 40 Ma. During the drifting period, a number of mafic alkaline intrusions, including kimberlites and related rocks, intruded across southern Africa. Two distinct intrusion peaks have been reported at 145–115 and 95–80 Ma, corresponding to kimberlite Group II and I, respectively (e.g. Smith *et al.* 1985; Basson & Viola 2004).

In the study area a wide range of Cenozoic sedimentary deposits cover the low coastal plain (Fig. 1). Raised marine terraces occurring at various elevations along the coast have been linked to Miocene, Pliocene and Quaternary transgressions (Pether 2000).

Geomorphology

The SW African high-elevated passive margin comprises a gently inclined low coastal plain and an elevated inland plateau separated by a seaward-facing escarpment (the 'Great Escarpment' of King 1953) (Fig. 2).

In the southern part of the study area (Fig. 2), the low-lying coastal plain [from 0 to 200 m asl (above sea level) in altitude and up to 80 km wide], is

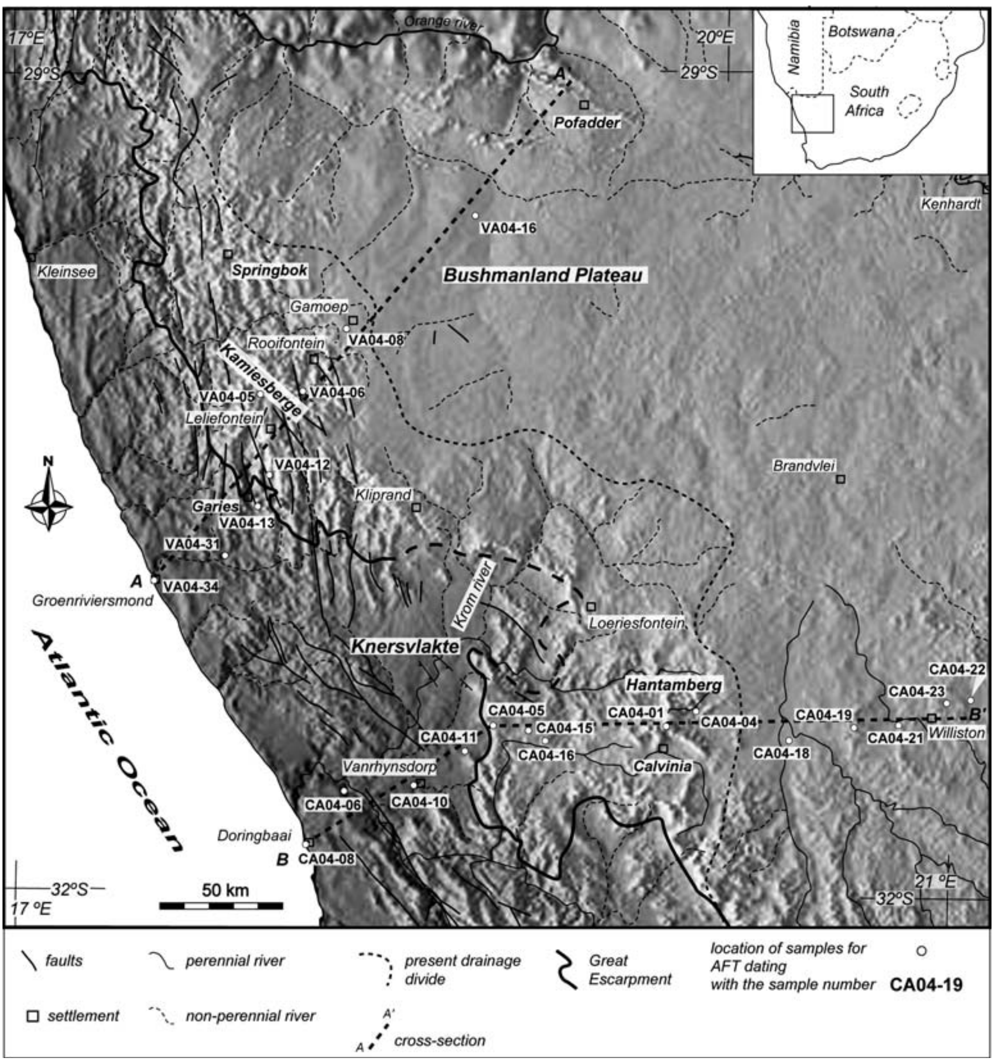

Fig. 2. Shaded relief map of the study area (western South Africa) with the locations of the analysed samples.

developed mainly across the Gariep and Vanrhynsdorp (Nama) Group phyllites and siltstones (Johnson *et al.* 2006) (Fig. 1). Close to the coast, isolated remnants of quartzite-dominated rocks of Cape Supergroup (Johnson *et al.* 2006) also crop out.

Inland, the coastal plain is flanked by a well-defined escarpment that, near Vanrhynsdorp, forms an approximately 600 m-high, subvertical cliff. The summit of the escarpment is capped by up to 50 m of subhorizontal Table Mountain Group quartzites and quartz-conglomerates. To the north, the top of the escarpment cliff gradually loses altitude, and in the area known as the Knersvlakte (Fig. 2) the quartzite cap disappears and the escarpment is morphologically much less pronounced. Here, in places, it is eroded by the Krom River and its tributaries (Kounov *et al.* 2008, Fig. 2).

East of the escarpment the inland plateau has a mean elevation of about 1000 m and generally low relief (Fig. 2). The top of the plateau is underlain by the Karoo Supergroup siliciclastic sediments (Johnson *et al.* 2006) intruded by numerous subhorizontal Mid-Jurassic Karoo dolerite sills and several subvertical dykes (Fig. 1). Small hills (kopies), formed by the relatively resistant dolerite sills, rise locally above the plateau floor. For example, in the area around Calvinia (*c.* 1000 m) a number of these high kopies, with densely spaced dolerites and steep scarps, rise up to 700 m above the general plateau (e.g. Hantamberg: Fig. 2).

The landscape of the northern part of the study area (Namaqualand) is defined by three main geomorphic units: an approximately 50 km-wide sandy coastal plain; an approximately 30-km wide escarpment zone; and an internal elevated plateau (the Bushmanland Plateau) at a mean altitude of 950 ± 50 m (Fig. 2). The escarpment here is much less defined from a geomorphological perspective than further to the south. Indeed, it lacks a proper scarp and is, instead, represented by a broad highland region, which includes the Kamiesberge Mountains, reaching up to 1770 m in altitude (Fig. 2). The Namaqualand area is underlain by the high-grade granitic gneisses and granulites of the Mesoproterozoic Namaqua Metamorphic Province (Johnson *et al.* 2006) (Fig. 1).

Structures

The large-scale Mesozoic–Cenozoic structural grain of the west coast of South Africa is characterized by complex sets of faults. In the Namaqualand area two major sets of faults strike N to NNW and NW, respectively. They can be easily identified on satellite and aerial images, especially along the escarpment area and in the elevated plateau, which is not covered by Quaternary deposits (Fig. 3). Most of these faults show top-to-the-west normal displacement, but small-scale thrusts and grabens that strike N to NNW have also been documented (Brandt *et al.* 2005; Viola *et al.* 2005). Several major north–south-trending normal faults juxtapose the Late Palaeozoic Nama Group sediments against the metamorphic basement rocks of the Namaqualand Metamorphic Province (Fig. 1). It is generally difficult to constrain precisely the age of these faults because of the common lack of marker horizons. Nevertheless, the fault structures above the escarpment in the Namaqualand area have been described broadly as late Mesozoic–Cenozoic based on the age of the rocks they dissect (Brandt *et al.* 2005; Viola *et al.* 2005). Significant lateral variation in the depth of denudation owing to post-Cretaceous normal faulting has been recognized in Namaqualand (Brown 1992). Neotectonic activity along these structures is indicated by a large number of seismic events recorded in the region (e.g. Viola *et al.* 2005).

Apatite fission-track analysis

Fission-track results

In this section we present AFT data from two traverses that run roughly east-west and, thus, perpendicular to the trend of the Great Escarpment in the region (location shown in Figs 1 & 2).

Analytical procedures for AFT analysis follow those outlined by Seward (1989). Etching of the apatite grains was carried out with 7% HNO_3 at 21 °C for 50 s. Irradiation was carried out at the ANSTO facility, Lucas Heights, Australia. Microscopic analysis was completed at University of Cape Town using an optical microscope with a computer-driven stage (‘Autoscan’ software from Autoscan Systems Pty Ltd, Melbourne, Australia). All ages were determined using the zeta approach (Hurford & Green 1983) with a zeta value of 341 ± 10 for CN5 (Table 1, analyst: A. Kounov). They are reported as central ages (Galbraith & Laslett 1993) with a 1σ error (Table 1). The magnification used was 1250×, at which horizontal confined track lengths and etch-pits diameters (D_{par}) were also measured. Between 5 and 10 etch pits were measured per dated grain, depending on the quality and the density of the track pits on the grain surface. The D_{par} values of the analysed samples are between 1.6 and 2.7 μm, with the average relative error of less than 5%.

Our northernmost traverse, between Groenriviersmond and Pofadder, is located within the gneissic basement of the Namaqua Metamorphic Province (Fig. 1) and is referred here to as the Namaqua Traverse. Our southern traverse, referred to as the Karoo Traverse, between Doringbaai and

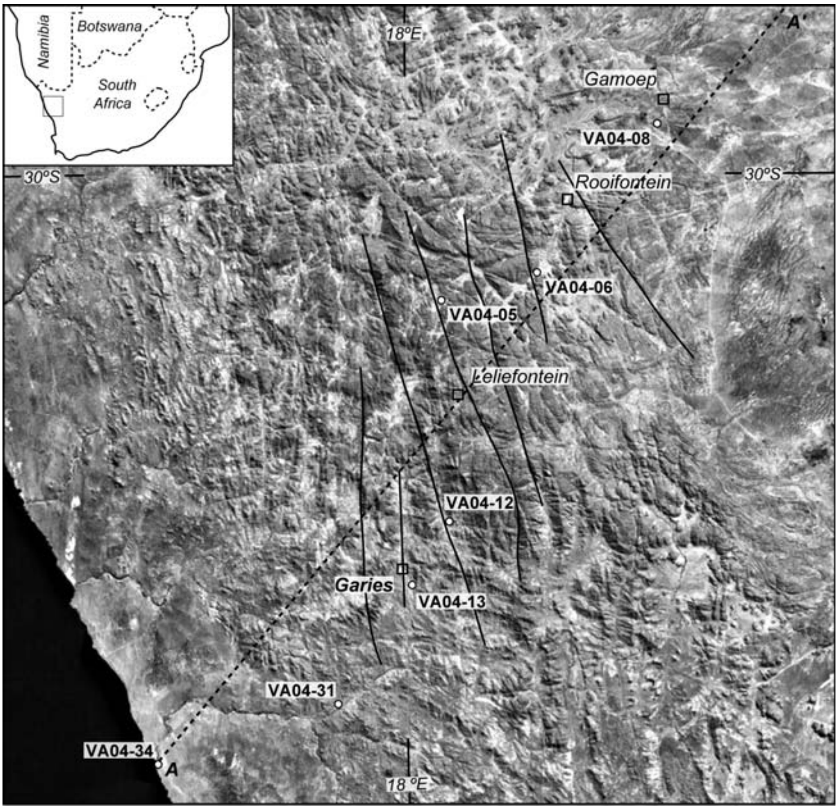

Fig. 3. Landsat image of the Namaqualand area with interpreted traces of the steep fault structures shown in Figure 4. Many other lineaments, probably corresponding to Mesozoic faults, are also easily visible. Line A–A′ trace the section of Figure 4.

Williston, crosses the Gariep and Nama Group sediments, as well as the Cape and Karoo Supergroup deposits and Karoo dolerites (Fig. 1). The locations of the samples are shown in Figure 1 and summarized in Table 1.

The stratigraphic age of the 22 analysed samples ranges from Precambrian (Namaqua metamorphics) through to early Jurassic (Karoo dolerites; Table 1). Samples yield AFT ages ranging between 180 and 86 Ma, with the older ages characteristic for the continental interior above the escarpment (Fig. 1). All samples passed the χ^2 test and have AFT ages significantly younger than their stratigraphic ages, indicating that they were affected by temperatures between 60 and 110 °C or higher after their deposition or formation (Green & Duddy 1989; Corrigan 1993). The samples have mean track lengths between 12.3 and 14.54 μm, with a standard deviation of 0.88–2.41 μm (Table 1). Samples with less than 35 measured track lengths were not taken into further consideration because of their low number of confined track measurements, insufficient for a robust modelling approach.

Samples with the youngest AFT ages (114–86 Ma) show mostly narrow, unimodal track-length distributions (standard deviation 0.88–1.48 μm) and lack short tracks (<*c.*11 μm: Fig. 4). This suggests that they experienced fast cooling from temperatures higher than about 110 °C along a rather simple cooling path at the time indicated by the AFT age (Laslett *et al.* 1987). Track-length distributions for the older samples are, instead, significantly different. Histograms show generally broader distributions (standard deviation 1.24–2.41 μm) with ‘tails’ of shorter tracks (<*c.* 11 μm: Fig. 4). This indicates that these samples experienced a more complex thermal history during which they spent a significant amount of time at temperatures between about 110 and 60 °C (apatite partial annealing zone) before final exhumation, which caused a shortening of their old tracks (Green & Duddy 1989; Corrigan 1993).

Table 1. *Apatite fission-track results*

Sample number	Latitude (S)/ Longitude (E)	Altitude (m)	Lithology	Stratigraphic division	Number of grains	$\rho_d(N_d)$ (10^6 cm^{-2})	$\rho_s(N_s)$ (10^6 cm^{-2})	$\rho_i(N_i)$ (10^6 cm^{-2})	$P(\chi^2)$ (%)	U (conc.) (ppm)	Central age ($\pm 1\sigma$) (Ma)	MTL ($\pm 1\sigma$) (μm)	SD (N) (μm)	D_{par} (μm)
Namaqua Traverse														
VA04/34	S30.85997/E17.57692	20	Bi gneiss	NMP	17	1.118 (4687)	2.703 (467)	4.949 (855)	98.8	61	103.3 ± 6.8	14.06 ± 0.12	1.12 (86)	2.2
VA04/31	S30.76619/E17.88967	104	Bi gneiss	NMP	23	1.079 (4146)	0.415 (250)	0.709 (427)	99.9	9	106.8 ± 9.2	14.29 ± 0.10	0.93 (86)	2.3
VA04/13	S30.59236/E18.00863	224	granitic gneiss	NMP	22	1.003 (4217)	2.771 (1926)	4.119 (2863)	81.7	51	114.0 ± 5.1	13.79 ± 0.31	1.14 (102)	2.1
VA04/12	S30.48478/E18.05954	420	granitic gneiss	NMP	17	0.968 (4146)	1.254 (410)	1.985 (649)	99.94	29	103.4 ± 7.4	14.54 ± 0.25	1.48 (36)	2.4
VA04/05	S30.19328/E18.04745	1010	charnockite	NMP	22	1.250 (4306)	2.646 (1309)	4.433 (2193)	90.92	44	125.9 ± 6.1	13.72 ± 0.12	1.24 (102)	1.7
VA04/06	S30.15173/E18.21009	840	granitic gneiss	NMP	13	1.092 (4306)	3.790 (621)	5.103 (836)	99.92	61	136.8 ± 8.5	13.42 ± 0.25	1.57 (39)	1.6
VA04/08	S29.93714/E18.40922	960	charnockite	NMP	21	1.052 (4306)	2.317 (1530)	2.771 (1830)	96.97	35	148.3 ± 7.1	12.32 ± 0.22	2.41 (123)	1.6
VA04/16	S29.52382/E18.93592	940	gneiss	NMP	22	1.017 (4687)	1.389 (902)	2.141 (1391)	99.93	27	111.5 ± 6.0	14.04 ± 0.12	1.35 (128)	2.3
Karoo Traverse														
CA04/08	S31.81319/E18.23548	1	sandstone	TMG	13	1.003 (4217)	1.259 (353)	1.619 (454)	88.54	22	131.6 ± 10.3	12.42 ± 0.61	2.10 (12)	2.3
CA04/06	S31.63409/E18.40824	35	sandstone	VG	13	0.997 (4292)	1.366 (411)	2.352 (707)	43.35	37	98.0 ± 7.3	12.59 ± 0.45	0.91 (4)	2.1
CA04/10	S31.60948/E18.70766	102	sandstone	VG	22	0.956 (4306)	1.029 (707)	1.939 (1332)	99.9	27	86.0 ± 4.9	13.87 ± 0.09	0.88 (102)	2.2
CA04/11	S31.48021/E18.92288	259	gravel	VG	22	12.141 (4292)	0.691 (492)	1.500 (1067)	79.77	18	94.7 ± 6.0	13.89 ± 0.13	1.27 (101)	2.2
CA04/05	S31.37293/E19.01697	825	conglomerate	TMG	26	10.505 (4217)	0.874 (729)	1.251 (1044)	88.77	18	123.9 ± 7.3	13.76 ± 0.25	1.65 (44)	2.5
CA04/15	S31.39204/E19.18904	774	dolerite	Karoo magm.	22	11.418 (4292)	0.347 (264)	0.545 (414)	100	6	122.9 ± 10.5	14.76 ± 0.57	1.8 (10)	2.7
CA04/16	S31.43291/E19.26326	808	conglomerate	Dwyka Gp	23	9.772 (4446)	1.368 (1092)	2.408 (1922)	42.74	30	94.2 ± 4.9	13.84 ± 0.12	1.21 (101)	2.2
CA04/01	S31.38068/E19.78422	1520	dolerite	Karoo magm.	31	11.697 (4217)	0.254 (220)	0.277 (240)	100	3	180.3 ± 17.9	14.36 ± 0.24	1.27 (28)	2.5
CA04/04	S31.32342/E19.91601	1080	dolerite	Karoo magm.	22	1.269 (4306)	0.757 (474)	1.186 (743)	76.16	12	136.6 ± 9.2	13.35 ± 0.26	1.98 (56)	2
CA04/18	S31.43123/E20.30881	1024	sandstone	Ecca Gp	20	1.068 (4446)	1.500 (492)	2.628 (861)	99.51	31	103.1 ± 6.7	13.28 ± 0.39	1.29 (11)	2.2
CA04/19	S31.38337/E20.59016	1187	dolerite	Karoo magm.	15	0.947 (4446)	0.319 (132)	0.396 (163)	98.54	5	128.7 ± 15.6	14.79 ± 0.23	0.46 (4)	3.1
CA04/21	S31.35553/E20.79923	1036	sandstone	Ecca Gp	15	0.974 (4687)	1.979 (419)	2.524 (534)	97.89	34	128.7 ± 9.4	13.58 ± 0.24	1.52 (42)	2.3
CA04/23	S31.28741/E20.99069	1192	dolerite	Karoo magm.	20	0.997 (4306)	0.308 (150)	0.392 (191)	99.87	5	131.8 ± 9.2	15.78 ± 0.34	0.758 (5)	2.7
CA04/22	S31.26801/E21.0839	1100	sandstone	Ecca Gp	21	1.214 (4146)	1.309 (552)	2.102 (886)	85.02	21	127.7 ± 8.1	13.38 ± 0.13	1.31 (95)	2.5

All ages are central ages (Galbraith 1981). $\lambda D = 1.55125 \times 10^{-10}$. A geometry factor of 0.5 was used. Zeta $= 341 \pm 10$ for CN5 glass. Irradiations were performed at the ANSTRO facility, Lucas Heights, Australia. $P(\chi^2)$ is the probability of obtaining χ^2 values for ν degrees of freedom, where ν= number of crystals -1. ρ_d, ρ_s and ρ_i represent the standard, sample spontaneous and induced track densities, respectively. MTL is the mean track length. SD is the standard deviation. D_{par} is the mean track pit length. NMP, Namaqua Metamorphic Province; TMG, Table Mountain Group; VG, Vanrhynsdorp Group; Dwyka Gp, late Carboniferous–early Permian (Karoo Supergroup); Ecca Gp, Permian (Karoo Supergroup); Karoo magm., Karoo magmatics (*c*. 183 Ma, Duncan *et al*. 1997).

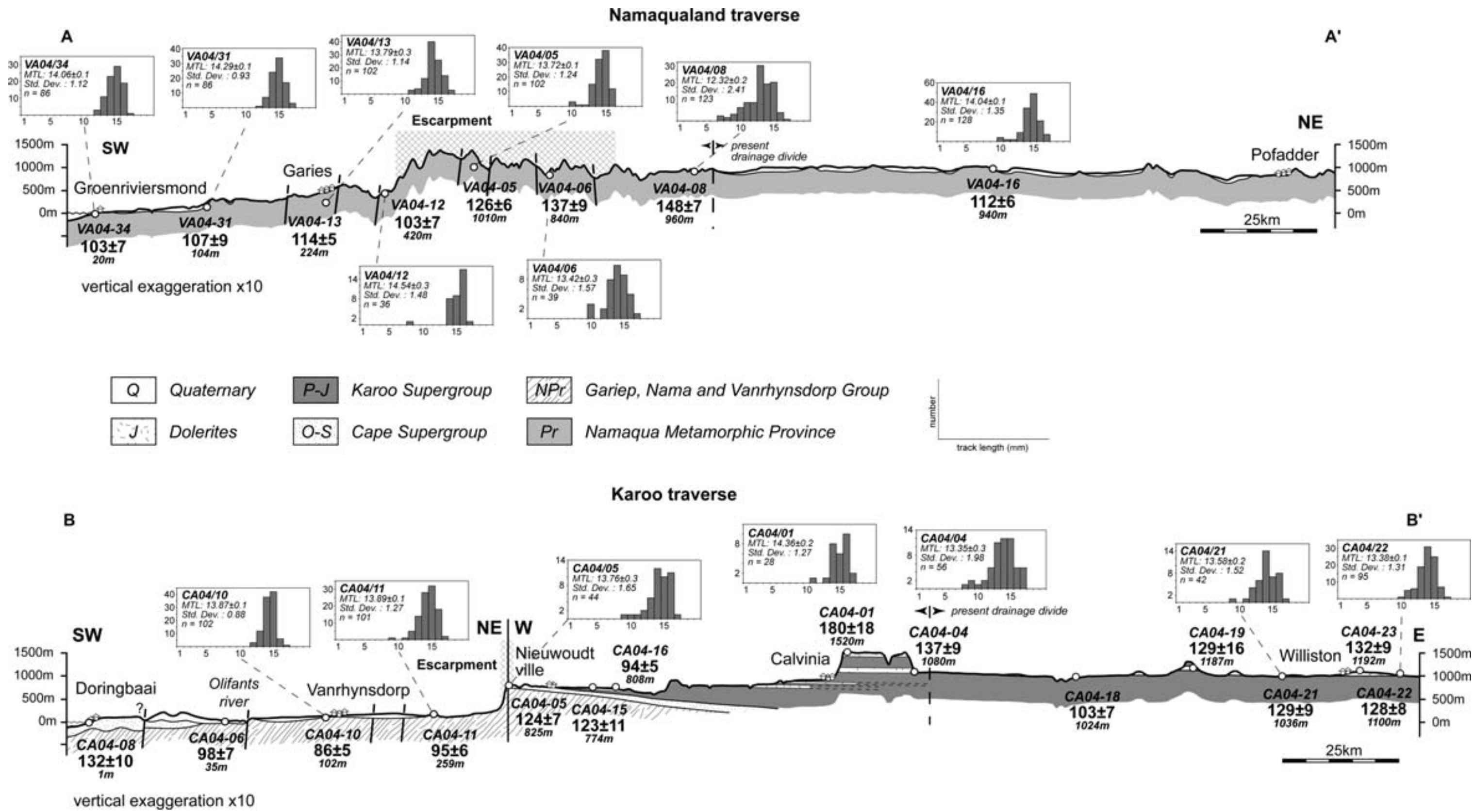

Fig. 4. Cross-sections A–A′ between Groenriviersmond and Pofadder (Namaqua Traverse) and B–B′ between Doringbaai and Williston (Karoo Traverse) with the locations of apatite fission-track samples, relative ages and track-length distribution histograms.

Namaqua Traverse. Along this traverse eight samples from crystalline rocks of the Namaqua Metamorphic Province were analysed. Apatite ages range from 148 ± 7 to 103 ± 7 Ma. Samples show a strong correlation between age and distance from the coast, with age increasing systematically towards the interior of the continent (Figs 4 & 5). Two minor exceptions are samples VA04/12 and VA04/16 (Figs 4 & 5). The age–altitude plot for this traverse shows some disturbance (Fig. 5).

Karoo Traverse. This traverse contains two samples from the Palaeozoic Table Mountain Group, three from the Neoproterozoic Vanrhynsdorp Group, four from the Karoo Group sediments (including the Dwyka and Ecca formations) and five from Early Jurassic Karoo dolerites (Table 1). Apatite ages range from 180 ± 18 to 86 ± 5 Ma. The youngest samples, characterized by longer mean-track lengths, are found on the coastal plain (Figs 4 & 5). Three exceptions are samples CA04/08, CA04/16 and CA04/18. The correlation plots between age and distance from the coast and altitude appear disturbed (Fig. 5). The topographically highest sample (a dolerite dyke, CA04/01) yields an AFT age of 180 ± 18 Ma that corresponds closely to its presumed emplacement age (*c.* 183 Ma, $^{40}Ar/^{39}Ar$ age: Duncan *et al.* 1997) (Fig. 4).

Apatite fission-track thermal modelling

Fission tracks in apatites are formed continuously through time at an approximately uniform initial length. Upon heating, tracks are then gradually annealed or shortened to a length that is determined by the maximum temperature to which apatites are exposed and the time. For example, tracks are completely annealed at a temperature of 110–120 °C for a period of 10^5–10^6 years. These annealing characteristics allow the construction of time–temperature paths by inverse modelling.

We have modelled our AFT data to quantify the timing and amount of cooling at specific locations along the studied traverses. Modelling of the apatite age and track-length distribution data was carried out with the program Monte Trax by Gallagher (Gallagher 1995), using an initial track length of 16.3 μm. Age and track-length distribution parameters, as well as user-defined time (t)–temperature (T) boxes, are used as input data, allowing just one change of direction of the t–T path within each individual t–T box. To select t–T points and define a cooling path, the program uses a Genetic Algorithm probabilistic approach

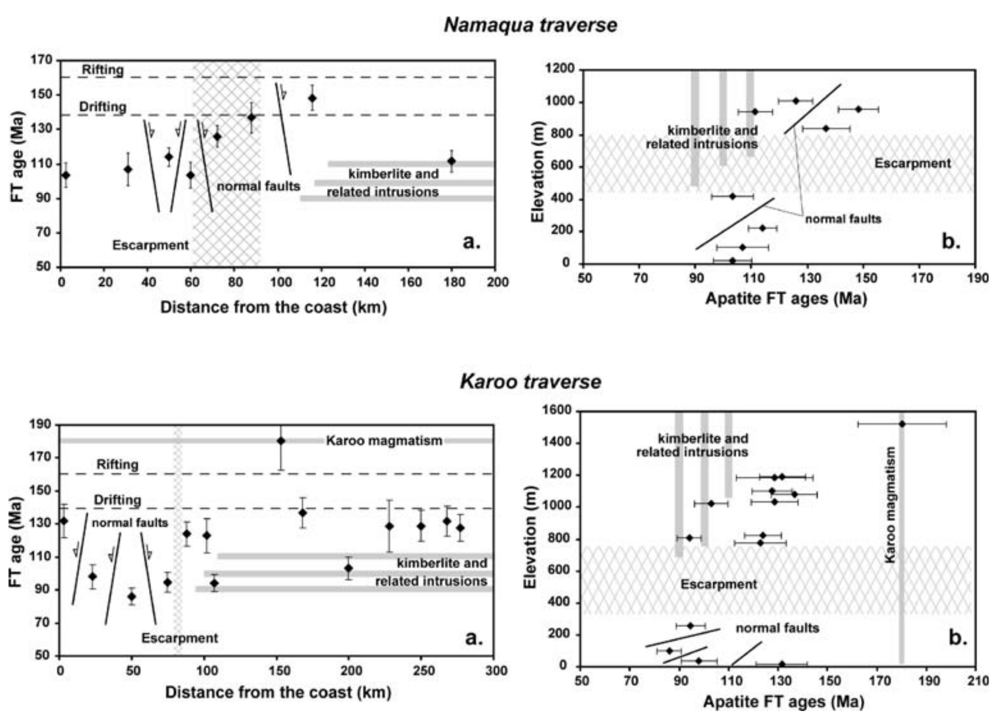

Fig. 5. Relationship between apatite fission-track ages from the Namaqualand and Karoo traverses v. (**a**) distance from the coast and (**b**) elevation.

(Gallagher & Sambridge 1994), which optimizes the stochastic production of successive generations of thermal history models. The predicted fission-track parameters are then quantitatively compared to the observed (measured) values, and the level of consistency between the two sets is used to choose the thermal history that is most consistent with the observed data. It is important to remember that the best thermal history obtained during this process is not necessarily the only possible. Other thermal histories may match the observed data similarly well and it is therefore imperative to consider as many other geological constraints as possible to determine the most likely path.

It has been shown that the annealing properties of apatites are controlled principally by their chlorine/fluorine ratio (e.g. Green *et al.* 1986; Ketcham *et al.* 1999; Barbarand *et al.* 2003). Given that a positive correlation has been demonstrated between Cl wt% and apatite D_{par} (Donelick 1993), we have systematically measured apatite track etch-pit diameters (Table 1). Most of the samples modelled in our study have D_{par} values between 2.0 and 2.5 μm (Table 1). This is close to the value that we have obtained for the Durango apatite standard (2.36 ± 0.02 μm; $n = 100$) etched under the same conditions used for the rest of our samples. The composition of Durango apatite was therefore used with the Laslett algorithm in our models (Laslett *et al.* 1987). Samples VA04/05, VA04/06 and VA04/08, which have D_{par} values lower than those measured for the Durango apatite (between 1.6 and 1.7 μm, Table 1), may have been annealed at temperatures lower than those indicated by the models. The net amount of denudation would in this case be overestimated by modelling, but the timing of individual cooling events would instead remain unaffected. These samples were therefore also used for the modelling.

In order to discard the possibility that variations in AFT ages may be due to variable apatite compositions and not to different thermal histories, we have plotted the measured D_{par} against the corresponding AFT ages. The lack of any positive correlation along the traverses suggests that the compositional influence is negligible (Fig. 6). Moreover, no particular positive correlation between the age and D_{par} is found when individual grain measurements are plotted. In eight samples (out of 22 samples analysed) a positive correlation is shown but with R^2 values (coefficient of determination) less than 0.1. Only four samples show R^2 values between 0.1 and 0.3.

Modelling results from our study are illustrated in Figure 7.

Namaqua Traverse. Modelling of the AFT data along this traverse has to take into account the

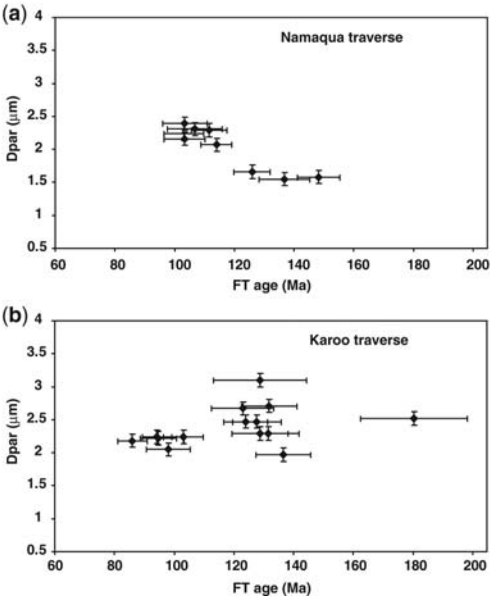

Fig. 6. Apatite fission-track ages plotted against D_{par} values for individual samples from (**a**) the Namaqua and (**b**) the Karoo traverses. No correlation is present.

uncertainty concerning the pre-rift thermal history of the samples and especially of those above the escarpment. The age (114–103 Ma) and track-length distribution (mean track lengths between 13.9 and 14.54 μm) of the samples collected along the coastal plain (Fig. 4) suggest that they cooled from temperatures higher than 110 °C at the time indicated be their AFT age, thus only after the opening of the South Atlantic.

The last known significant thermal event affecting this area was linked to the late Neoproterozoic Pan-African orogeny. The time of the post-orogenic cooling is not known. Most probably the Namaqualand area was covered by the Permo-Triassic Karoo deposits, but their areal extent and their local maximum thickness are not known. All these uncertainties in the pre-rift thermal history of the samples above the escarpment makes the modelling a serious challenge. We therefore allowed a large degree of freedom for the pre-rifting (pre-150 Ma) thermal conditions in our models and applied tighter time–temperature constraints only for the last 150 Ma time window. Input time–temperature boxes were defined for three main time intervals: 150–120 Ma, 120–80 Ma and 80–0 Ma (Fig. 7). These periods overlap with phases of accelerated cooling in Southern Africa reported by previous studies (Brown *et al.* 2002; Raab *et al.* 2002; Tinker *et al.* 2008).

The results for samples both above and below the escarpment show one distinct period of fast

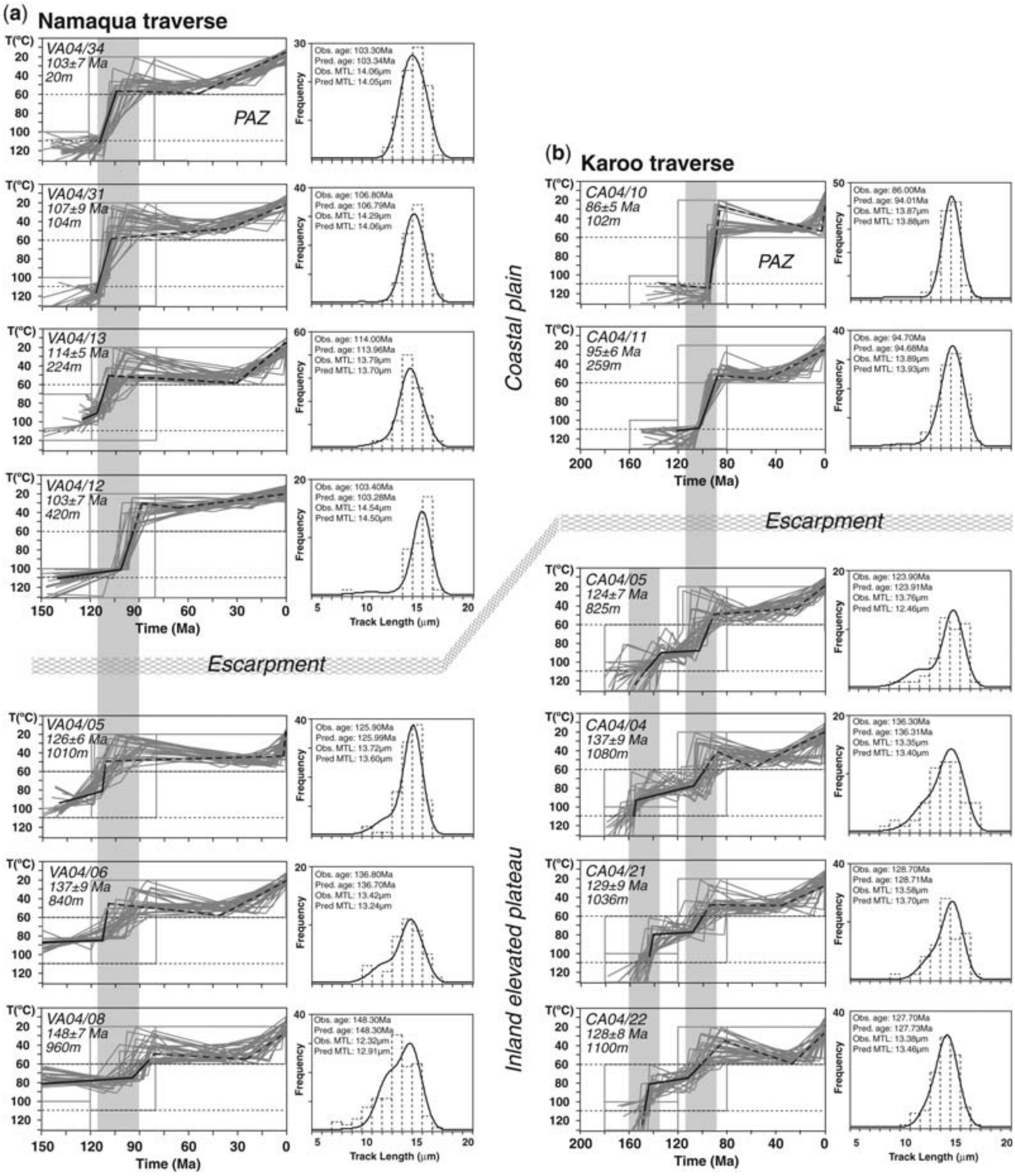

Fig. 7. Modelled thermal histories for samples, and comparison between the predicted fission-track parameters and the observed data from (**a**) the Namaqualand and (**b**) the Karoo traverses with their AFT age and altitude. The shaded vertical bands represent the cooling events at 160–138 Ma and 115–90 Ma. Horizontal dashed lines within individual models at 60–110 °C bracket the partial annealing zone (PAZ) for apatite within the temperature limits assigned by Laslett *et al.* (1987). The thick black lines represent the best-fit paths, and the grey lines the best 50 modelled paths. The dashed segments of the thermal histories at temperatures lower than 60 °C indicate only a possible continuation of the thermal history because the annealing model is not sufficiently sensitive below 60 °C.

cooling between 115 and 90 Ma. Before 115 Ma the samples above the escarpment underwent a very slow cooling between 90 and 80 °C, whereas the samples from the coastal plain were still at temperatures higher than 110 °C.

Karoo Traverse. AFT ages from this traverse are interpreted as being fully reset during the Karoo igneous event (*c.* 180 Ma: Duncan *et al.* 1997). Based on zircon fission-track analysis, Brown *et al.* (1994) suggested maximum palaeotemperatures of at least 250 ± 50 °C at about 190 ± 10 Ma for the Karoo sediments. Time–temperature constrains identical to those used in the Namaqua traverse were adopted as input to the model of the samples above the escarpment. This allows the program to search for possible changes of direction in the time–temperature path within three main intervals: 150–120 Ma, 120–80 Ma and 80–0 Ma (Fig. 7). Considering their age and track-length distribution (Fig. 4), the samples from the coastal plain were fully reset before 150 Ma.

Modelling from this traverse reveals two distinct cooling events (Fig. 7). The first one is between 160 and 138 Ma, and is recorded only by the samples above the escarpment. This first cooling event is followed by a period of quiescence during which the samples above the escarpment were at temperatures of between 80 and 90 °C for at least 30 Ma (Fig. 7).

Similar to the results from the Namaqua traverse, a period of rapid cooling between 115 and 90 Ma is indicated by these models (Fig. 7). This event is recorded by samples both above and below the escarpment. The fact that the samples from the coastal plain record just this event also suggests that they were at temperatures higher than 110 °C before 115 Ma.

Discussion

Denudation history

As shown above, our AFT analysis reveals two discrete phases of cooling, separated by a period of relative thermal stability.

160–138 Ma. This cooling event is constrained only by the thermal models of the samples situated inland from the present escarpment in the Karoo Traverse (Fig. 7). It is still not clear whether this event represents post-Karoo magmatism (*c.* 180 Ma) thermal relaxation or is, instead, the expression of tectonic processes related to rifting. The fact that the thermal models from the Namaqua Traverse above the escarpment show no evidence of significant cooling during this same time interval suggests that the thermal history of the samples from the Karoo Basin was, indeed, affected by the widespread Karoo magmatism (Fig. 7). We favour, therefore, a scenario whereby this cooling episode is linked to post-Karoo thermal relaxation. Most probably, all samples situated landward from the present escarpment were part of a stable continental interior during this period and, therefore, were not significantly affected by the tectonic and/or thermal processes related to the rifting itself.

It is not possible to reconstruct the thermal history of the samples along the present coastal plain during this period by AFT analysis because they were at temperatures higher than the AFT closure temperature at this time (Fig. 7).

138–115 Ma. Modelling of samples from the continental interior indicates this to be a period of quiescence, during which these rocks experienced cooling of less than 15 °C during *c.* 30 Ma (Fig. 7). This time coincides with the transition of the south Atlantic margin from an active, related to the rifting, to a passive mode (e.g. Nürnberg & Müller 1991).

The distinctly younger ages of samples situated above the escarpment (between 94 ± 6 and 112 ± 6 Ma: Fig. 4) are difficult to explain (e.g. CA04/16 and CA04/18 from the Karoo Traverse, and VA04/16 from the Namaqua Traverse). Although most of the previously published AFT ages from the elevated continental interior are older than 150 Ma, some scattered younger ages are also reported (Brown *et al.* 1990, 2000; Gallagher & Brown 1999). The lack of any particular patterns in their distribution and evidence for active post-rifting tectonics exclude the possibility that these data are related to major post-rifting denudation events. Nevertheless, Gallagher & Brown (1999) suggested that significant post-break-up denudation in the present-day continental interior could be possibly the result of ‘structural reactivation’ along unidentified tectonic lineaments.

It is also possible that these young ages are the result of the chemistry of the dated minerals, which allowed for much lower closure temperatures (hence the young ages), or that they are due to heating from local kimberlitic intrusions (Fig. 5). Two distinct peaks of several hundreds of intrusions have been reported from southern Africa at 145–115 and 95–80 Ma (e.g. Basson & Viola 2004; Trumbull *et al.* 2007).

The modelling of two samples from the coastal plain (VA04/13 and VA04/12) and one from the escarpment area (VA04/05) (Fig. 7) along the Namaqualand Traverse also suggests relatively slow cooling during this period. AFT analysis does not allow the presence of possible differences in the amount of denudation to be established between the coast and the continental interior.

115–90 Ma. All modelled samples show a distinct second episode of accelerated cooling between 115 and 90 Ma. In particular, most of the samples from the coastal plane cooled from temperatures above 110 °C (Fig. 7). If the geothermal gradient is known, it is possible to estimate the amount of denudation for each sample. The present-day geothermal gradient in the Karoo Basin is about 20 °C km^{-1} (Gough 1963). Brown *et al.* (2002) and Tinker *et al.* (2008) derived palaeo-geothermal gradients of 20–25 °C km^{-1} for the Middle Cretaceous in Southern Africa from AFT analysis on borehole samples. Given the difficulties in constraining palaeo-geothermal gradients, however, we limit ourselves here to a rough estimation of the patterns of denudation along the two traverses for the period 115–90 Ma for three possible different palaeo-geothermal gradients: 20, 25 and 30 °C km^{-1} (Fig. 8). Considering the lithological difference of the samples analysed along the two traverses, one could assume that high geothermal gradients are more probable for the Namaqua Traverse, underlined entirely by gneissic rock. Nevertheless, such a possible difference would not affect the differential denudation between the coastal plain and the continental interior or across some of the tectonic structures observed along the two traverses.

Figure 8 suggests that there is a substantial difference in the amount of denudation between the coastal plain and the elevated plateau in the period 115–90 Ma. The amount of denudation ranges from a maximum of 1.5–2.7 km along the coast to less than 1 km above the escarpment for each of the selected geothermal gradients. Moreover, along the Namaqualand traverse denudation changes significantly and abruptly across individual faults within the faulted area. This suggests a prolonged tectonic activity during or subsequent to this period that affected both the coastal plain and the present day escarpment area (Figs 2 & 3) and is confirmed by the disturbed age–altitude plot for the same traverse (Fig. 5).

Sample VA04/12 was collected from within the footwall of a large normal fault (Fig. 2), mapped on the 1 000 000 geological map of South Africa (Keyser 1998) and was easily visible on satellite images (Fig. 3). Thermal modelling for this sample predicts fast cooling between 100 and 90 Ma, thus slightly later than for the other samples. We suggest that this may reflect the time of faulting (Fig. 7). Active tectonics along the coastal area could be responsible for an elevated geothermal gradient. However, even for an elevated geothermal gradient (30 °C km^{-1}), the estimated denudations from the coast and the escarpment area are significantly higher than the maximum calculated denudation for the elevated plateau (Fig. 8).

It is not clear whether the differential denudation observed between the coastal plain and the plateau along the Karoo Traverse is in part also due to faulting, as shown for the case of the Namaqua Traverse. There are no observed or mapped faults in the escarpment area of the southern traverse, although several faults are mapped along the coastal plain and the age–altitude plot shows some disturbance (Fig. 5). Top-to-the-west normal faulting could explain the relatively old age of sample CA04/08 (132 ± 10 Ma) collected at the coast (Figs 1 & 4). Differential uplift related to flexural isostatic rebound along the coast due to the enhanced denudation should also be considered. Irrespective of whether accompanied by tectonic movements or not, the large difference in the amount of denudation between the coastal plain and the continental interior must be a direct consequence of differential erosion. High denudation along the coast was probably the result of significant erosion by high-energy river systems that flowed down to the low Atlantic base level from a drainage divide, which, already at this time, coincided with the present-day position of the escarpment (as previously suggested along the south African margin by Cockburn *et al.* 2000; Brown *et al.* 2002; Tinker *et al.* 2008). It must be pointed out that the erosion along the coastal plain was probably facilitated by the presence of the Gariep and Vanrhynsdorp (Nama) Group phyllites and siltstones. The continental interior was instead eroded slowly possibly by low-energy river systems, a difference that explains the substantial change in the amount of denudation across the escarpment (Fig. 8).

Other evidence for the regional character of the substantial increase in denudation and uplift during the Mid-Cretaceous is as follows. (1) the Early Cretaceous Rietport granite (133.9 ± 1.3 Ma: De Beer *et al.* 2002), intruded in the coastal area, was already exhumed close to the surface by the end of the Palaeocene, as suggested by the presence of high-level olivine melilitite plugs intruded into the granite at around 56 Ma (De Beer *et al.* 2002). (2) Increased Mid-Cretaceous denudation has already been reported by other low-temperature thermochronological studies on the western South African margin (e.g. Brown *et al.* 1990, 2000). (3) A significant amount of uplift was also observed offshore Namaqualand, where seismic profiles and boreholes show significant erosional horizons marking the Aptian regression (121–112 Ma; e.g. Gerrard & Smith 1983; Brown *et al.* 1995) (Fig. 9). From the Aptian until the end of the Turonian (*c.* 90 Ma), increasing amounts of offshore clastic deposits and other minor unconformities are reported (Gerrard & Smith 1983; Paton *et al.* 2007) (Fig. 9). (4) Hirsch (2008) recently reported a second rifting phase from 117 to 95 Ma deduced from subsidence analysis in the Orange Basin. This rifting phase was related to subsidence in the outer shelf contemporaneous with uplift in the inner shelf. This observation is consistent with the tectonically induced uplift of the continental margin during the same period suggested here. (5) In western Central Namibia, the regional-scale Waterberg thrust, which brought the Neoproterozoic Damara basement over Jurassic sandstones, may also indicate an important, Mid-Cretaceous

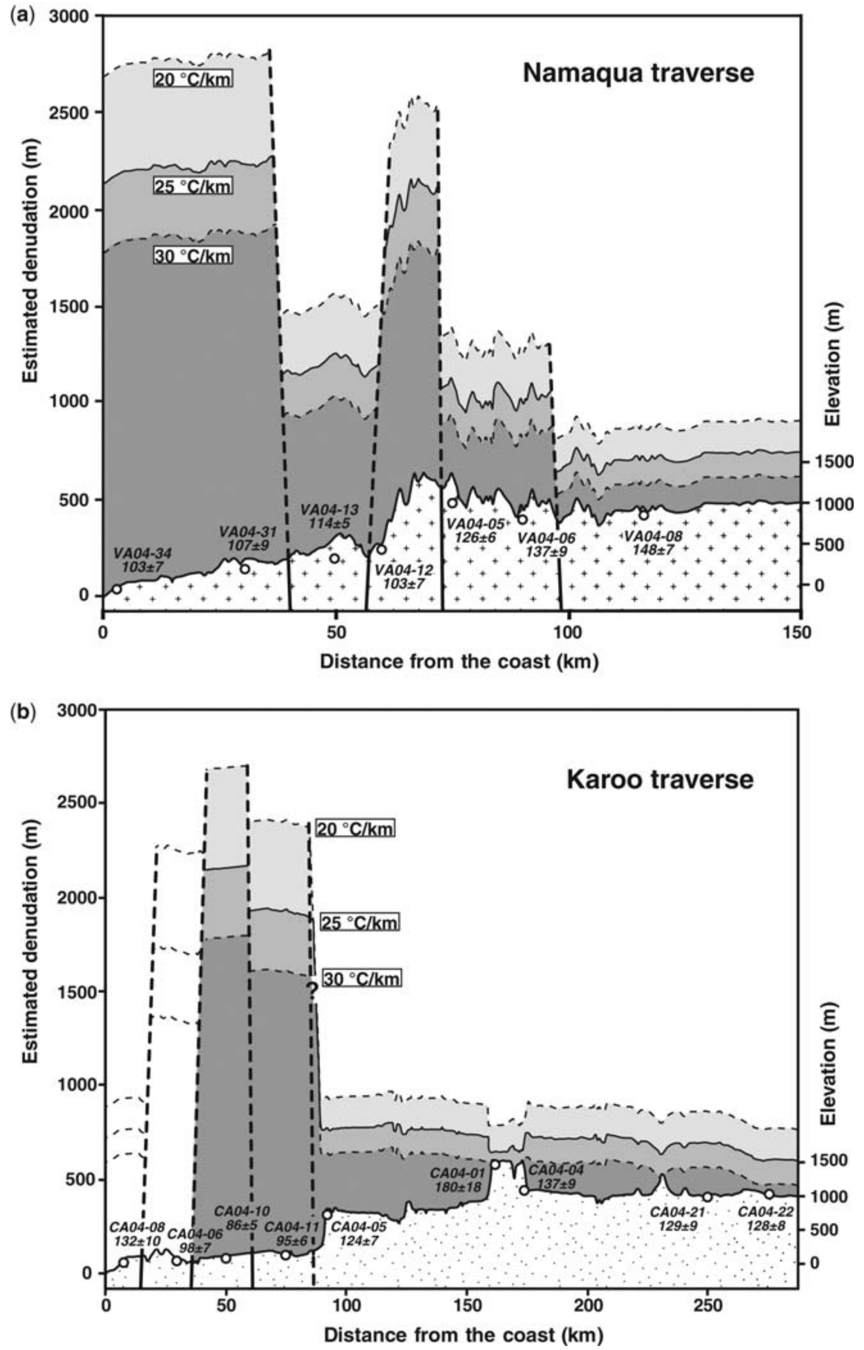

Fig. 8. Estimated denudation for the period between 115 and 90 Ma calculated from AFT data modelling and based on three possible palaeo-geothermal gradients of 20, 25 and 30 °C km^{-1} for: (**a**) the Namaqualand Traverse and (**b**) the Karoo Traverse. For samples CA04/06 and CA04/08 from the Karoo Traverse the presented dashed lines for the estimated denudation are only suggested. The samples were not modelled because of the insufficiency of the track length records.

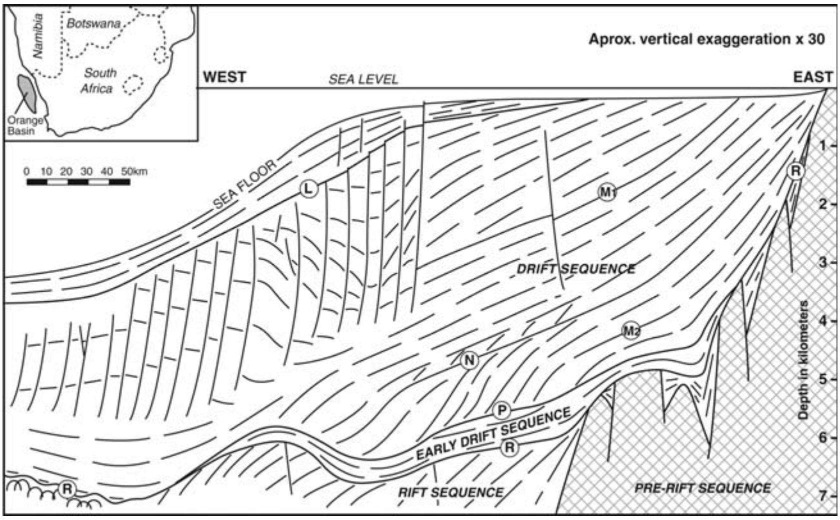

Fig. 9. Diagrammatic section across Orange Basin based on well and seismic data (from Gerrard & Smith 1983). Main unconformities: R, drift onset unconformity (Valanginian); P, Aptian unconformity; L, base Tertiary unconformity. Secondary unconformities: M_2, Albian; N, Cenomanian; M_1, Coniacian.

episode of crustal shortening and uplift (cf. Raab *et al.* 2002; Viola *et al.* 2005 and references therein).

Collectively, these data support a model of significant Mid-Cretaceous uplift and denudation along the western South African margin. The demonstrated significant changes in amount of denudation between the continental interior and its margin are here tentatively related to the fact that already at that time the drainage divide was located close to its present position, thus separating high-energy river systems rapidly eroding the coastal area from low-energy systems developed in the elevated plateau. These observations allow us to suggest that it is probably during this time that most of South African present-day topography was established (see also Doucouré & de Wit 2003; de Wit 2007).

Post-90 Ma. The post Mid-Cretaceous denudation of the study area cannot be constrained by AFT analysis because, by then, the sampled rocks were already exhumed to crustal levels corresponding to temperatures lower than 60 °C, thus beyond the resolution of the method. Nevertheless, some authors have reported the existence of a Late Cretaceous phase of accelerated denudation based on fission-track analysis from other areas, such as the Drakensberg Mountains (Brown *et al.* 2002) and northern Namibia (Raab *et al.* 2002, 2005).

Much lower rates for the present-day denudation in southern Africa are estimated from cosmogenic nuclides analysis (e.g. Fleming *et al.* 1999; Cockburn *et al.* 2000; Brown *et al.* 2002; Kounov *et al.* 2007). Whilst some extrapolate low denudation rates to the entire Cenozoic on the basis of the prevailing aridity of the climate and the lack of substantial uplift throughout that period (e.g. Cockburn *et al.* 2000), other authors consider the Cenozoic as the main period of uplift, topographic development and escarpment formation in Southern Africa (e.g. Partridge & Maud 1987; Partridge 1998; Burke 1996).

Whilst there is still no consensus on this, our study allows us to conclude with confidence that:

- Cenozoic denudation in the study area was less than 2–3 km because it did not bring to the surface rocks from deeper crustal levels (e.g. there are no samples with fission-track ages younger than Late Cretaceous);
- present-day erosional rates are at least an order of magnitude lower than during the Cretaceous (e.g. Kounov *et al.* 2007).

In addition, offshore seismic stratigraphy has revealed deposition of up to 2 km of sediments along the western African margin since the Mid-Cretaceous, suggesting substantial subsidence during this time as well as considerable onshore denudation. On the other hand, much thinner Tertiary succession occurs above a significant unconformity (Gerrard & Smith 1983; Brown *et al.* 1995; Aizawa *et al.* 2000; Paton *et al.* 2007) Tinker *et al.* 2008) (Fig. 9). This unconformity is described as a well-developed marine planation surface witnessing the uplift of the offshore margin (Aizawa *et al.* 2000). Nevertheless, it must be mentioned that the mean annual sediment input along the SW coast of Africa (as measured by sediment accumulation rates in the main Orange Basin depocentre) decreased progressively from the late Cretaceous to the Neogene (Dingle & Hendey 1984; Rust & Summerfield 1990). This decrease is confirmed by the observation that Late Cretaceous lake sediments can still be found as crater deposits infilling the craters of Cretaceous olivine melilites and kimberlites in the Namaqualand area above the escarpment (de Wit 1999).

We suggest that Cenozoic pulses of uplift and denudation have existed and played a role in the development of the main geomorphological features of the passive margin, although less important than those during the Cretaceous,

Evidence of Cenozoic, and even Quaternary, tectonics, including fault reactivation and sedimentation, have indeed been reported both offshore and onshore Namaqualand and Southern Namibia by a number of authors (e.g. Andreoli *et al.* 1996; Brandt *et al.* 2005; Viola *et al.* 2005).

Driving mechanism for the Mid-Cretaceous denudation

The AFT results presented in this study reveal the existence of a distinct period of active tectonic uplift accompanied by denudation between 115 and 90 Ma on the western coast of South Africa. Tectonically driven pulses of accelerated denudation have already been reported from the Southern Africa passive margin (Brown 1992; Brown *et al.* 2002; Raab *et al.* 2002). Although their existence is now well documented by low-temperature thermochronology analysis and by offshore seismic and borehole data, their driving forces remain still largely unknown (Gerrard & Smith 1983; Brown *et al.* 1995, 2002; Aizawa *et al.* 2000).

Gilchrist & Summerfield (1990) were the first to suggest that flexural isostatic rebound, resulting from the high denudation rate on the evolving coast flank of the rifted margin, may have played a significant role in the margin upwarp. They demonstrated that this process could generate 600 m of uplift on the Southern African margin, and estimated the total denudation along the coast to be between 2 and 3 km. Although this mechanism may have been important during margin development, it cannot explain the 5 km denudation across the Southern African margin since continental break-up that has been reported in previous AFT studies, nor the tectonically induced pulses of denudation (Brown *et al.* 1990; Raab *et al.* 2002, 2005).

Some authors claim that climate changes could induce uplift (e.g. Molnar & England 1990; Wobus *et al.* 2003), whereas others support exactly the opposite view, suggesting that tectonic processes could result in climate changes (e.g. Raymo & Ruddiman 1992; Burbank *et al.* 2003). During the Cretaceous Southern Africa was characterized by hot climatic conditions, whereas in the Middle Miocene the cold Benguela current led to a more arid climate (e.g. Uenzelmann-Neben *et al.* 2007 and references therein). Several studies suggest that this cold and arid climate prevailed for a significant part of the Cenozoic (e.g. Cockburn *et al.* 2000). It is, however, unlikely that the dramatic decrease in denudation rates (an order of magnitude) observed from the Cretaceous–Cenozoic boundary (e.g. Cockburn *et al.* 2000; Brown *et al.* 2002; Tinker *et al.* 2008) was controlled only by climate changes. More recent analogues are also against such a theory. For example, present-day denudation rates in the Drakensberg escarpment area (Fleming *et al.* 1999), which is characterized by humid and warm environment, are similar to those reported for the west coast of southern Africa, where climatic conditions are, instead, significantly dry (Cockburn *et al.* 2000; Van der Wateren & Dunai 2001). Also, Cenozoic denudation rates from the western coast of Southern Africa are similar to those reported for the same period in Madagascar and Sri Lanka, where warm and humid climate conditions have prevailed since the Cretaceous (Hewawasam *et al.* 2003; Seward *et al.* 2004; Vanacker *et al.* 2007).

In summary, all of these observations suggest that an important acceleration in denudation rate could have been caused only by a significant regional uplift, with climate-driven erosion acting only as a second-order factor.

Some authors relate post-break-up tectonic processes in Southern Africa to dynamic processes in the mantle (Doucouré & de Wit 2003; Burke 1996; de Wit 2007; Tinker *et al.* 2008). Burke (1996) suggested that the highlands of Southern Africa are mainly Cenozoic in age (possibly as young as 30 Ma), whereas other authors present evidence that much of the present topography was formed during the Cretaceous (Doucouré & de Wit 2003; de Wit 2007; Kounov *et al*. 2008). They all agree, however, that substantial uplift is probably associated with the tomographically imaged low-velocity zone in the lower mantle–core boundary, called the African Superswell (e.g. Lithgow-Bertelloni & Silver 1998). According to this dynamic topography model, present-day topography would be a dynamic feature formed in response to vertical stresses at the base of the Southern African lithosphere that generated positive buoyancy in the mid–lower mantle.

We believe that this scenario accounts efficiently for the results and observations of our paper and also of other recent AFT studies (Brown *et al.* 2002; Raab *et al.* 2002; Tinker *et al.* 2008).

Tinker *et al.* (2008) correlated periods of increased denudation with peaks of kimberlite emplacement, and the formation of the Parana and Agulhas igneous provinces, thus suggesting a causative link between lower-mantle upwelling processes and increased denudation. Certainly, peaks of kimberlitic activity were related to the emplacement of hot magma at the base of the lithosphere, which triggered diffuse crustal uplift. This large-scale uplift was accompanied by tectonic activity probably related to reactivation of fault structures along the continental margin.

Conclusions

AFT results across the western coast of South Africa and its interior reported in this paper are consistent with the existence of a discrete, tectonically induced, Mid-Cretaceous pulse of substantial denudation. Thermal modelling of the new fission-track data indicates up to 2.5 km of denudation in the coastal zone and less than 1 km on the elevated interior plateau during this phase of accelerated denudation. Greater tectonic activity occurred along the passive margin and its interior during this period than in the Cenozoic. This suggests that the Mid-Cretaceous was probably the time when most of the present-day Southern African high-elevation topography was formed.

The spatial patterns of denudation reported here suggest localized, post-rifting and fault-controlled uplift along the passive margin.

It is tentatively suggested that the substantial Mid-Cretaceous pulse of denudation is a direct consequence of significant uplift associated with the African Superswell, a tomographically imaged low-velocity zone at the lower-mantle–core boundary.

This work was supported by the Claude Leon Foundation post-doctoral fellowship (to Alexandre Kounov) and by Inkaba yeAfrica funds. Fission-track dating was carried out at the University of Cape Town (UCT). We would like to thank M. Tredoux for providing a Macintosh computer for the fission-track laboratory at UCT. Constructive reviews by A. Henk and an anonymous reviewer, and the editorial work of F. Lisker helped to improve the quality of the paper. This is AEON contribution 68, and Inkaba yeAfrica contribution number XX.

References

AIZAWA, M., BLUCK, B., CARTWRIGHT, J., MILNER, S., SWART, R. & WARD, J. 2000. Constrains on the geomorphological evolution of Namibia from the offshore stratigraphic record. *Communs of the Geological Survey of Namibia*, **12**, 337–346.

ANDREOLI, M. A. G., DOUCOURÉ, M., VAN BEVER DONKER, J., BRANDT, D & ANDERSEN, N. J. B. 1996. Neotectonics of Southern Africa – a review. *Africa Geoscience Review*, **3**, 1–16.

BARBARAND, J., CARTER, A., WOOD, I. & HURFORD, T. 2003. Compositional and structural control of fission-track annealing in apatite. *Chemical Geology*, **198**, 107–137.

BASSON, I. & VIOLA, G. 2004. Passive kimberlite intrusion into actively dilating dyke-fracture arrays: evidence from fibrous calcite veins and extensional fracture cleavage. *Lithos*, **76**, 283–297.

BRANDT, D., ANDREOLI, M. & MCCARTHY, T. S. 2005. The Late Mesozoic paleosoils and Cenozoic fluvial deposits at Vaalputs, Namaqualand, South Africa. Possible depositional mechanism and their bearing on the evolution of the continental margin. *South African Journal of Geology*, **108**, 267–280.

BROWN, L. F., BENSON, J. M. *ET AL.* 1995. *Sequence stratigraphy in Offshore South African divergent basins, an atlas on exploration for Cretaceous Lowstand Traps by SOEKOR (Pty) Ltd.* AAPG Studies in Geology, **41**.

BROWN, R. W. 1992. *A Fission Track Thermochronology Study of the Tectonic and Geomorphic Development of the Sub-aerial Continental Margins of Southern Africa.* PhD thesis, La Trobe University, Melbourne, Australia.

BROWN, R. W., GALLAGHER, K. & DUANE, M. 1994. A quantitative assessment of the effects of magmatism on the thermal history of the Karoo sedimentary sequence. *Journal of African Earth Sciences*, **18**, 227–243.

BROWN, R. W., GALLAGHER, K., GLEADOW, A. J. W. & SUMMERFIELD, M. A. 2000. Morphotectonic evolution of the South Atlantic margins of Africa and South America. *In*: SUMMERFIELD, M. A. (ed.) *Geomorphology and Global Tectonics.* Wiley, Chichester, 255–284.

BROWN, R. W., RUST, D. J., SUMMERFIELD, M. A., GLEADOW, A. J. W. & DE WIT, M. C. J. 1990. An Early Cretaceous phase of accelerated erosion on the south-western margin of Africa: Evidence from apatite fission track analysis and the offshore sedimentary record. *Nuclear Tracks and Radiation Measurement*, **17**, 339–350.

BROWN, R. W., SUMMERFIELD, M. A. & GLEADOW, A. J. W. 2002. Denudation history along a transect across the Drakensberg Escarpment of southern Africa derived from apatite fission track thermochronology. *Journal of Geophysical Research*, **107,** (B12), 2350, doi:10.1029/2001JB000745.

BURBANK, D. W., BLYTHE, A. E. *ET AL.* 2003. Decoupling of erosion and precipitation in the Himalayas. *Nature*, **426**, 652–655.

BURKE, K. 1996. The African Plate. *South African Journal of Geology*, **99**, 341–409.

COCKBURN, H. A. P., BROWN, R. W., SUMMERFIELD, M. A. & SEIDL, M. A. 2000. Quantifying passive margin denudation and landscape development using a combined fission-track thermochronometry and cosmogenic isotope analysis approach. *Earth and Planetary Science Letters*, **179**, 429–435.

CORRIGAN, J. D. 1993. Apatite fission-track analysis of Oligocene strata in South Texas, USA; testing annealing models. *Chemical Geology*, **104**, 227–249.

COX, K. G. 1992. Karoo igneous activity and the early stages of the break-up of Gondwanaland. *In*: STOREY, B. C., ALABASTER, T. & PANKHURST, R. J. (eds) *Magmatism and the Causes of Continental Break-up*. Geological Society, London, Special Publications, **68**, 137–148.

DE BEER, C. H., GRESSE, P. G., THERON, J. N. & ALMOND, J. E. 2002. *The Geology of the Calvinia Area. Explanation of 1:250 000-scale Sheet 3118 Calvinia*. Council for Geoscience, South Africa.

DE WIT, M. C. J. 1999. Post-Gondwana drainage and the development of diamond placers in Western South Africa. *Economic Geology*, **94**, 721–740.

DE WIT, M. J. 2007. The Kalahari Epeirogeny and climate change: differentiating cause and effect from core to space. *South African Journal of Geology*, **110**, 367–392.

DE WIT, M. J. & RANSOME, I. G. D. (eds) 1992. Regional inversion tectonics along the southern margin of Gondwana. *Inversion Tectonics of the Cape Fold Belt, Karoo and Cretaceous Basins of Southern Africa*. Balkema, Rotterdam, 15–21.

DINGLE, R. V. & HENDEY, B. Q. 1984. Late Mesozoic and Tertiary sediment supply to the eastern Cape basin (SE Atlantic) and paleo-drainage system in southwestern Africa. *Marine Geology*, **56**, 13–26.

DONELICK, R. A. 1993. Apatite etching characteristics versus chemical composition. *Nuclear Tracks and Radiation Measurements*, **21**, 604.

DOUCOURÉ, C. A. & DE WIT, M. J. 2003. Old inherited origin for the present near bimodal topography of Africa. *Journal of African Earth Sciences*, **36**, 371–388.

DUNCAN, R. A., HOOPER, P. R., REHACEK, J., MARSH, J. S. & DUNCAN, A. R. 1997. The timing and duration of the Karoo igneous event, southern Gondwana. *Journal of Geophysical Research*, **102**, 18 127–18 138.

DU TOIT, A. 1926. *Geology of South Africa*. Oliver & Boyd, Edinburgh.

EAGLES, G. 2007. New angles on South Atlantic opening. *Geophysical Journal International*, **166**, 353–361.

EALES, H. V., MARCH, J. S. & COX, K. G. 1984. The Karoo igneous province: an introduction. *In*: ERLANK, A. J. (ed.) *Petrogenesis of the Volcanic Rocks of the Karoo Province*. Geological Society of South Africa, Special Publications, **13**, 1–26.

FLEMING, A., SUMMERFIELD, M. A., STONE, J. O. H., FIFIELD, L. K. & CRESSWELL, R. G. 1999. Denudation rates for the southern Drakensberg escarpment, SE Africa, derived from in-situ-produced cosmogenic ^{36}Cl: initial results. *Journal of the Geological Society, London*, **156**, 209–212.

GALBRAITH, R. F. 1981. On statistical-models for fission track counts. *Journal of the International Association for Mathematical Geology*, **13**, 471–478.

GALBRAITH, R. F. & LASLETT, G. M. 1993. Statistical models for mixed fission-track ages. *Nuclear Tracks and Radiation Measurements*, **21**, 459–470.

GALLAGHER, K. 1995. Evolving temperature histories from apatite fission-track data. *Earth and Planetary Sciences Letters*, **136**, 421–435.

GALLAGHER, K. & SAMBRIDGE, M. 1994. Genetic algorithms: A powerful tool for large-scale nonlinear optimization problems. *Computational Geosciences*, **20**, 1229–1236.

GALLAGHER, K. & BROWN, R. 1999. The Mesozoic denudation history of the Atlantic margins of southern Africa and southeast Brazil and the relationship to offshore sedimentation. *In*: CAMERON, N. R., BATE, R. H. & CLURE, V. S. (eds) *The Oil and Gas Habitats of the South Atlantic*. Geological Society, London, Special Publications, **153**, 41–53.

GALLAGHER, K., BROWN, R. & JOHNSON, C. 1998. Fission track analysis and its applications to geological problems. *Annual Review of Earth and Planetary Science*, **26**, 519–572.

GERRARD, I. & SMITH, G. C. 1983. Post-Paleozoic succession and structure of the southwestern African continental margin. *In*: WATKINS, J. S. & DRAKE, C. L. (eds) Studies in Continental Margin Geology. *AAPG*, *Memoir*, **34**, 49–74.

GILCHRIST, A. R. & SUMMERFIELD, M. A. 1990. Differential denudation and flexural isostasy in formation of rifted-margin upwarps. *Nature*, **346**, 739–742.

GILCHRIST, A. R., HENK, K. & BEAUMONT, C. 1994. Post-Gondwana geomorphic evolution of southwestern Africa: Implications for the controls on landscape development from observations and numerical experiments. *Journal of Geophysical Research*, **99**, 12 211–12 228.

GOUGH, D. I. 1963. Heat flow in the Southern Karoo. *Proceedings of the Royal Society of London, Series A*, **272**, 207–230.

GREEN, P. F. & DUDDY, I. R. 1989. Some comments on paleotemperature estimation from apatite fission track analysis. *Journal of Petroleum Geology*, **12**, 111–114.

GREEN, P. F., DUDDY, I. R., GLEADOW, A. J. W., TINGATE, P. R. & LASLETT, G. M. 1986. Thermal annealing of fission tracks in apatite, 1. A qualitative description. *Chemical Geology*, **59**, 237–253.

GRESSE, P. G. 1995. The Late Pan-African Vanrhynsdorp foreland thrust-fold belt in southern Namaqualand, South Africa. *Journal of African Earth Sciences*, **21**, 91–105.

HAWKESWORTH, C., KELLEY, S., TURNER, S., LE ROEX, A. & STOREY, B. 1999. Mantle processes during Gondwana break-up and dispersal. *Journal of African Earth Sciences*, **28**, 239–261.

HEWAWASAM, T., VON BLANCKENBURG, F., SCHALLER, M. & KUBIK, P. 2003. Increase of human over natural erosion rates in tropical highlands constrained by cosmogenic nuclides. *Geology*, **31**, 597–600.

HIRSCH, K. 2008. Integrating structural and sedimentological observations with numerical lithospheric models to assess the 3D evolution of the South African continental passive margin. PhD Thesis, Free University, Berlin, Germany.

HURFORD, A. J. & GREEN, P. F. 1983. The zeta age calibration of fission-track dating. *Chemical Geology*, **41**, 285–317.

JOHNSON, M. R., ANHEAUSSER, C. R. & THOMAS, R. J. (eds) 2006. *The Geology of South Africa*. Geological Society of South Africa, Johannesburg.

JOURDAN, F., FÉRAUD, G., BERTRAND, H. & WATKEYS, M. K. 2007. From flood basalts to the inception of oceanization: Example from the 40Ar/39Ar high resolution picture of the Karoo large igneous province, *Geochemistry, Geophysics, Geosystems*, **8**, Q02002, doi:10.1029/2006GC001392.

KETCHAM, R. A., DONELICK, R. A. & CARLSON, W. D. 1999. Variability of apatite fission-track annealing kinetics III: Extrapolation to geological time scales. *American Mineralogist*, **84**, 1235–1255.

KEYSER, N. (compiler). 1998. *Geological Map of the Republic of South Africa, 1997* (released 1998). Council for Geoscience, Pretoria.

KING, L. C. 1953. Canons of landscape evolution. *Geological Society of America Bulletin*, **64**, 721–752.

KOUNOV, A., NIEDERMANN, S., DE WIT, M. J., VIOLA, G., ANDREOLI, M. & ERZINGER, J. 2007. Present denudation rates at selected sections of the South African escarpment and the elevated continental interior based on cosmogenic ^{3}He and ^{21}Ne. *South African Journal of Geology*, **110**, 235–248.

KOUNOV, A., VIOLA, G., DE WIT, M. J. & ANDREOLI, M. 2008. A Mid Cretaceous paleo-Karoo River Valley across the Knersvlakte plain (northwestern coast of South Africa): Evidence from apatite fission-track analysis. *South African Journal of Geology*, **111**, 409–420.

LASLETT, G. M., GREEN, P. F., DUDDY, I. R. & GLEADOW, A. J. W. 1987. Thermal annealing of fission tracks in apatite 2. A Quantitative Analysis. *Chemical Geology (Isotope Geoscience Section)*, **65**, 1–13.

LITHGOW-BERTELLONI, C. & SILVER, P. 1998. Dynamic topography, plate driving forces and the African superswell. *Nature*, **395**, 269–272.

MOLNAR, P. & ENGLAND, P. 1990. Late Cenozoic uplift of mountain ranges and global climate change: chicken or egg? *Nature*, **346**, 2934.

MOORE, A. & BLENKINSOP, T. 2006. Scarp retreat pinned drainage divide in the formation of the Drakensberg escarpment, southern Africa. *South African Journal of Geology*, **109**, 599–610.

MOORE, M. E., GLEADOW, A. J. W. & LOVERING, J. F. 1986. Thermal evolution of rifted continental margins: New evidence from fission tracks in basement apatites from southeastern Australia. *Earth and Planetary Science Letters*, **78**, 255–270.

NÜRNBERG, D. & MÜLLER, R. D. 1991. The tectonic evolution of the South Atlantic from late Jurassic to present. *Tectonophysics*, **191**, 27–53.

OLLIER, C. D. 1985. Morphotectonics of continental passive margins with great escarpment. *In*: MORISAWA, M. & HACK, J. T. (eds) *Tectonic Geomorphology*. Allen & Unwin, Boston, MA, 3–25.

OLLIER, C. D. & MARKER, M. E. 1995. The great escarpment of southern Africa. *Zeitschrift für Geomorphologie, Supplementband*, **54**, 37–56.

PARTRIDGE, T. C. 1998. Of diamonds, dinosaurs and diastrophism: 150 million years of landscape evolution in southern Africa. *South African Journal of Geology*, **101**, 167–185.

PARTRIDGE, T. C. & MAUD, R. R. 1987. Geomorphic evolution of southern Africa since the Mesozoic. *South African Journal of Geology*, **90**, 179–208.

PATON, D. A., DI PRIMO, R., KUHLMANN, G., VAN DER SPUY, D. & HORSFIELD, B. 2007. Insights into the petroleum system evolution of the southern Orange Basin, South Africa. *South African Journal of Geology*, **110**, 261–274.

PERSANO, C., STUART, F. M., BISHOP, P. & BARFOD, D. N. 2002. Apatite (U–Th)/He age constrains on the development of the Great Escarpment on the southeastern Australian passive margin. *Earth and Planetary Science Letters*, **200**, 79–90.

PETHER, J., ROBERTS, D. L. & WARD, J. D. 2000. Deposits of the West Coast. *In*: PARTRIDGE, T. C. & MAUD, R. R. (eds) *The Cenozoic of Southern Africa*. Oxford University Press, UK, 33–54.

RAAB, M. J., BROWN, R. W., GALLAGHER, K., CARTER, A. & WEBER, K. 2002. Late Cretaceous reactivation of major crustal shear zones in northern Namibia: constraints from apatite fission track analysis. *Tectonophysics*, **349**, 75–92.

RAAB, M. J., BROWN, R. W., GALLAGHER, K., WEBER, K. & GLEADOW, A. J. W. 2005. Denudational and thermal history of the Early Cretaceous Brandberg and Okenyenya igneous complexes on Namibia's Atlantic passive margin. *Tectonics*, **24**, TC3006, doi:10.1029/2004TC001688.

RABINOVICH, P. D. & LABRECQUE, J. 1979. The Mesozoic South Atlantic Ocean and evolution of its continental margin. *Journal of Geophysical Research*, **84**, 5973–6002.

RAYMO, M. E. & RUDDIMAN, W. F. 1992. Tectonic forcing of Late Cenozoic climate. *Nature*, **359**, 117–122.

RUST, D. J. & SUMMERFIELD, M. A. 1990. Isopach and borehole data as indicators of rifted margin evolution in southwestern Africa. *Marine and Petroleum Geology*, **7**, 277–287.

SEIDL, M. A., WEISSEL, J. K. & PRATSON, L. F. 1996. The kinematics and pattern of escarpment retreat across the rifted continental margin of SE Australia. *Basin Research*, **12**, 301–316.

SEWARD, D. 1989. Cenozoic basin histories determined by fission track dating of basement granites, South Island, New Zealand. *Chemical Geology*, **79**, 31–48.

SEWARD, D., GRUJIC, D. & SCHREURS, G. 2004. An insight into breakup of Gondwana: Identifying events through low-temperature thermochronology from basement rocks of Madagascar. *Tectonics*, **23**, TC3007, doi:10.1029/2003TC001556.

SMITH, C. B., ALLSOPP, H. L., KRAMERS, J. D., HUTCHINSON, G. & RODERICK, J. C. 1985. Emplacement ages of Jurassic-Cretaceous South African kimberlites by the Rb–Sr method on phlogopite and whole rock samples. *Transactions of the Geological Society of South Africa*, **88**, 249–266.

STERN, C. R. & DE WIT, M. J. 2004. Rocas Verdes ophiolite, southernmost South America: remnants of progressive stages of development of oceanic type crust in a continental back arc basin. *In*: DE DILEK, Y. & ROBINSON, P. T. (eds) *Ophiolites in Earth History*. The Geological Society, London, Special Publications, **218**, 665–683.

TINKER, J., DE WIT, M. & BROWN, R. 2008. Mesozoic exhumation of the southern Cape, South Africa, quantified using apatite fission track thermochronology, *Tectonophysics*, **455**, 77–93.

TRUMBULL, R. B., REID, D. L., DE BEER, C., VAN ACKEN, D. & ROMER, R. L. 2007. Magmatism and continental breakup at the west margin of southern Africa: A geochemical comparison of dolerite dikes from northwestern Namibia and the Western Cape. *South African Journal of Geology*, **110**, 477–502.

UENZELMANN-NEBEN, G., SCHLÜTER, P. & WEIGELT, E. 2007. Cenozoic oceanic circulation within the South African gateway: indications from seismic stratigraphy. *South African Journal of Geology*, **110**, 275–294, doi:10.2113/gssajg.110.2/3.275.

VANACKER, V., VON BLACKENBURG, F., HEWAWASAM, T. & KUBIK, P. W. 2007. Constraining landscape development of the Sri Lankan escarpment with cosmogenic nuclides in river sediment. *Earth and Planetary Science Letters*, **253**, 402–414.

VAN DER BEEK, P. A. & BRAUN, J. 1999. Controls on post-mid-Cretaceous landscape evolution in the southeastern highlands of Australia: Insights from numerical surface process models. *Journal of Geophysical Research*, **104**, 4945–4966.

VAN DER WATEREN, F. M. & DUNAI, T. J. 2001. Late Neogene passive margin denudation history- cosmogenic isotope measurements from the central Namib desert. *Global and Planetary Change*, **30**, 271–307.

VIOLA, G., ANDREOLI, M., BEN-AVRAHAMA, Z., STENGELD, I. & RESHEF, M. 2005. Offshore mud volcanoes and on land faulting in southwestern Africa: neotectonic implications and constraints on the regional stress field. *Earth and Planetary Science Letters*, **231**, 147–160.

WOBUS, C. W., HODGES, K. V. & WHIPPLE, K. X. 2003. Has focused denudation sustained active thrusting at the Himalayan topographic front? *Geology*, **31**, 861–864.